Eur Biophys J (2002) 31: 245–256
DOI 10.1007/s00249-002-0227-1

ARTICLE

**Monica X. Li · Erik J. Saude · Xu Wang
Joyce R. Pearlstone · Lawrence B. Smillie
Brian D. Sykes**

Kinetic studies of calcium and cardiac troponin I peptide binding to human cardiac troponin C using NMR spectroscopy

Received: 26 October 2001 / Accepted: 21 February 2002 / Published online: 6 June 2002

Abstract Ca^{2+} and human cardiac troponin I (cTnI) peptide binding to human cardiac troponin C (cTnC) have been investigated with the use of 2D $\{^1H,^{15}N\}$ HSQC NMR spectroscopy. The spectral intensity, chemical shift, and line-shape changes were analyzed to obtain the dissociation (K_D) and off-rate (k_{off}) constants at 30 °C. The results show that sites III and IV exhibit 100-fold higher Ca^{2+} affinity than site II ($K_{D(III,IV)} \approx 0.2$ μM, $K_{D(II)} \approx 20$ μM), but site II is partially occupied before sites III and IV are saturated. The addition of the first two equivalents of Ca^{2+} saturates 90% of sites III and IV and 20% of site II. This suggests that the Ca^{2+} occupancy of all three sites may contribute to the Ca^{2+}-dependent regulation in muscle contraction. We have determined a k_{off} of 5000 s^{-1} for site II Ca^{2+} dissociation at 30 °C. Such a rapid off-rate had not been previously measured. Three cTnI peptides, $cTnI_{34–71}$, $cTnI_{128–147}$, and $cTnI_{147–163}$, were titrated to Ca^{2+}-saturated cTnC. In each case, the binding occurs with a 1:1 stoichiometry. The determined K_D and k_{off} values are 1 μM and 5 s^{-1} for $cTnI_{34–71}$, 78 ± 10 μM and 5000 s^{-1} for $cTnI_{128–147}$, and 150 ± 10 μM and 5000 s^{-1} for $cTnI_{147–163}$, respectively. Thus, the dissociation of Ca^{2+} from site II and $cTnI_{128–147}$ and $cTnI_{147–163}$ from cTnC are rapid enough to be involved in the contraction/relaxation cycle of cardiac muscle, while that of $cTnI_{34–71}$ from cTnC may be too slow for this process.

Keywords Troponin C · Calcium binding · NMR · Kinetics

Abbreviations *TnC*: troponin C · *cTnC*: cardiac muscle TnC · *cNTnC*: N-domain of cardiac muscle TnC · *cCTnC*: C-domain of cardiac muscle TnC · *sTnC*: skeletal muscle TnC · *sNTnC*: N-domain of skeletal muscle TnC · *sCTnC*: C-domain of skeletal muscle TnC · *TnI*: troponin I · *cTnI*: cardiac muscle TnI · *sTnI*: skeletal muscle TnI · $cTnI_{34–71}$: cTnI peptide (residues 34–71) · $cTnI_{128–147}$: cTnI peptide (residues 128–147) · $cTnI_{147–163}$: cTnI peptide (residues 147–163) · *HSQC*: heteronuclear single-quantum coherence

Introduction

As the Ca^{2+}-binding member of the troponin complex, troponin C (TnC) plays a key role in the Ca^{2+} regulation of contraction/relaxation in striated muscle. Conformational changes in TnC induced by Ca^{2+} association/dissociation are believed to be transmitted through other thin filament proteins, troponin I, troponin T, tropomyosin, and actin, resulting in activation/inhibition of actomyosin ATPase and muscle contraction/relaxation (for reviews see Geeves and Holmes 1999; Gordon et al. 2000). Two isoforms of TnC exist in striated muscle, skeletal muscle troponin C (sTnC) and cardiac muscle TnC (cTnC). Both molecules are dumbbell-shaped (for a review see Gagné et al. 1998) with two domains, N- and C-, connected through a linker and comprise four EF-hand helix-loop-helix motifs as potential Ca^{2+}-binding sites (sites I–IV). Sites I and II are paired as a unit in the N-terminal half, and sites III and IV form another pair in the C-terminal half of the molecule. Sites III and IV are of relatively higher affinity for Ca^{2+} and also bind Mg^{2+}. Sites I and II are of lower affinity and are believed to be specific for Ca^{2+}. Site I in

Presented at the Royal Society Meeting *From Chemical to Physiological Mechanism*

Dedicated to Professor H. Gutfreund on the occasion of his 80th birthday

M.X. Li · E.J. Saude · X. Wang · J.R. Pearlstone
L.B. Smillie · B.D. Sykes (✉)
CIHR Group in Protein Structure and Function,
Department of Biochemistry,
University of Alberta, Edmonton,
Alberta, Canada T6G 2H7
E-mail: brian.sykes@ualberta.ca
Tel.: +1-780-4925460
Fax: +1-780-4920886

cTnC is unable to bind Ca^{2+} at physiological concentrations owing to key amino acid substitutions (van Eerd and Takahashi 1975). Current evidence indicates a largely structural role for the C-domain, whose sites would be occupied by Ca^{2+}/Mg^{2+} throughout the contraction/relaxation cycle. The regulatory role is considered to be associated with the conformational changes induced by the association and dissociation of Ca^{2+} from N-domain sites I and II of sTnC or site II of cTnC.

The fundamental difference between sTnC and cTnC is that the binding of Ca^{2+} to sTnC is coupled by a large structural "opening" (Gagné et al. 1995), while the association of Ca^{2+} with cTnC results in minimal conformational changes (Sia et al. 1997; Spyracopoulos et al. 1997). This is mainly due to the fact that both sites I and II are functional in sTnC (Sheng et al. 1992), while only site II is active in cTnC (Putkey et al. 1989). The exposed hydrophobic surface in the Ca^{2+}-saturated sTnC has long been proposed (Herzberg et al. 1986) and has subsequently been proven (McKay et al. 1997, 1999) as the sTnI binding site. The significant reduction in the hydrophobic surface exposure of Ca^{2+}-saturated cTnC suggested that the mode of interaction between cTnC-cTnI may be different than that between sTnC-sTnI. However, we have found that both the regulatory domains of sTnC and cTnC adopt similar "open" conformations when bound to their respective TnI regions ($sTnI_{115–131}$ and $cTnI_{147–163}$) (Li et al. 1999; Spyracopoulos et al. 2000). This region of TnI has been identified by many biological and biophysical studies to be the region responsible for binding to the regulatory domain of TnC and this interaction modulates the interaction between the N-terminal ($sTnI_{1–40}$ and $cTnI_{34–71}$) and the inhibitory regions ($sTnI_{96–115}$ and $cTnI_{128–147}$) of TnI and TnC (for reviews see Farah and Reinach 1995; Solaro and Rarick 1998). Thus, the sequence of events involved in initiating skeletal and cardiac muscle contraction are actually very similar. However, the kinetics and thermodynamics of these events must differ for the two systems to account for the different physiological behavior of the two muscle types (for discussions see McKay et al. 2000; Pearlstone et al. 2000).

To understand the unique delicate energetic balance that exists for each system, it is important to study the time scales of Ca^{2+} binding and release from TnC, the accompanied structural changes, and the subsequent interactions of TnI with TnC. A number of studies have been performed on the kinetics of Ca^{2+} binding to TnC, isolated or in the troponin complex. There are major differences between the skeletal and cardiac isoforms. In sTnC, Ca^{2+} binding to sites I/II appears to be diffusion limited ($k_{on} \approx 10^8\ M^{-1}\ s^{-1}$) with a Ca^{2+} dissociation rate (k_{off}) of ~400–500 s^{-1} and the conformational change occurs almost simultaneously with the Ca^{2+} association/dissociation (Johnson et al. 1994; Rosenfeld and Taylor 1985a, 1985b). In cTnC, although Ca^{2+} binding to site II is also diffusion limited ($k_{on} \approx 10^8\ M^{-1}\ s^{-1}$, $k_{off} \approx 500–800\ s^{-1}$), the conformational change was found to be significantly slower than the Ca^{2+} on- and off-rates (Dong et al. 1996, 1997; Hazard et al. 1998). These reported on- and off-rates may not, however, represent the time scales of the molecular events that occur at physiological temperature (e.g. 37 °C in human heart), since most of these experiments were performed at 4 °C because Ca^{2+} kinetics become too fast to be measured by stopped-flow methods at temperatures higher than 4 °C (Hazard et al. 1998).

In the present work, we have systematically examined the kinetics of Ca^{2+} and three cTnI peptides ($cTnI_{34–71}$, $cTnI_{128–147}$, and $cTnI_{147–163}$) binding to cTnC at 30 °C with the use of 2D $\{^1H,^{15}N\}$ HSQC NMR spectroscopy. An advantage of NMR spectroscopy is that this technique can measure the time scales of the molecular events on proteins at temperatures close to physiological and can report information related to individual atoms throughout the sequence. Ca^{2+} and peptide titrations of sTnC and cTnC domains followed in detail by 2D $\{^1H,^{15}N\}$ HSQC NMR spectroscopy have been proven to be a powerful way of providing information such as binding stoichiometry, affinity, and energetics. For example, using this technique, we have previously characterized Ca^{2+} binding to sNTnC and sCTnC (Li et al. 1995; Mercier et al. 2000) and to cNTnC and an E41A mutant of sNTnC (Li et al. 1997). We also monitored the binding of $sTnI_{115–131}$ to sNTnC and E41A sNTnC (McKay et al. 1997, 2000), $cTnI_{147–163}$ to cNTnC (Li et al. 1999), $sTnI_{1–40}$ and $sTnI_{96–115}$ to sCTnC (Mercier et al. 2000), and $cTnI_{34–71}$ and $cTnI_{128–147}$ to cCTnC (Wang et al. 2001). In this study, the analysis of NMR spectral intensity, chemical shift, and line-shape changes induced by Ca^{2+} binding to cTnC and cTnI peptide binding to Ca^{2+}-saturated cTnC allow us to determine the dissociation (K_D) and off-rate (k_{off}) constants at 30 °C for these binding events. These measurements provide new insights into the time course of the important molecular events involved in the regulation of cardiac muscle contraction. In turn, it allows us to understand further the differences between cardiac and skeletal muscle contraction.

Materials and methods

Sample preparation

Recombinant human cTnC (residues 1–161) with the mutations C35S and C84S [denoted cTnC (C35S,C84S)] was used in this study. Since cTnC (C35S,C84S) is the only protein used throughout this work, (C35S,C84S) is omitted in this paper. The engineering of the expression vector of cTnC (C35S, C84S) was as follows: pET3a.cTnC(WT) was constructed as described previously (Pearlstone et al. 2000) and was used as the template for the construction of pET3a.cTnC(C35S,C84S); two rounds of mutagenesis (Stratagene) were performed using the paired 31-mer oligonucleotides 5′-GGCGCTGAGGATGGCAGCATCAGCACCAAGG-3′ and 5′-CCTTGGTGCTGATGCTGCCATCCTCAGCGCC-3′ for the C35S mutation and the paired 37-mer primers 5′-CCTGG TCATGATGGTTCGCAGCATGAAGGACGACAGC-3′ and 5′-GCTGTCGTCCTTCATGCTGCGAACCATCATGACCAGG-3′ for the C84S mutation (with base changes underlined). DNA

sequence analysis was used to confirm the correctness of all the mutants. The expression and purification of the ^{15}N-cTnC in BL21(DE3)pLysS cells were as described previously for ^{15}N-cNTnC (Li et al. 1997). Decalcification of ^{15}N-cTnC follows the procedure for ^{15}N-cNTnC (Li et al. 1997) except that 200 mM EDTA was used instead of 100 mM. A higher concentration of EDTA helps to remove the tightly bound metal ions in the C-domain of cTnC. Three synthetic cTnI peptides, $cTnI_{34–71}$, acetyl-AKKKSKISASRKLQLKTLLLQIAKQELEREAEERRG-EK-amide, $cTnI_{128–147}$, acetyl-TQKIFDLRGKFKRPTLRRVR-amide, and $cTnI_{147–163}$, acetyl-RISADAMMQALLGARAK-amide, respectively, were prepared using standard methodology for a typical TnI peptide (Tripet et al. 1997). The sequences were confirmed by amino acid analysis (Smillie and Nattriss 1990) and the mass verified by electrospray mass spectrometry. All NMR samples were 500 µL in volume. The buffer conditions were 100 mM KCl, 10 mM imidazole, 0.2 mM 2,2-dimethyl-2-silapentanesulfonic acid (DSS), and 0.01% NaN_3 in 90% H_2O/10% D_2O, and the pH was 6.9. The concentration of the apo ^{15}N-cTnC sample used for Ca^{2+} titration was determined to be 0.95 mM. The concentration of the ^{15}N-cTnC sample used for $cTnI_{34–71}$ titration followed by $cTnI_{147–163}$ was 0.80 mM and the ^{15}N-cTnC sample used for $cTnI_{128–147}$ titration was 0.56 mM. Each of the samples contains ~3–5 mM $CaCl_2$. A Gilson Pipetman P (model P2) was used to deliver the $CaCl_2$ solution and $cTnI_{34–71}$ and $cTnI_{128–147}$ peptide solutions for the titrations. Solid $cTnI_{147–163}$ was added during the titrations.

Ca^{2+} titration of ^{15}N-cTnC

Stock solutions of standardized 50 mM and 100 mM $CaCl_2$ in water were used for the titrations. To a NMR tube containing a 500 µL sample of 0.95 mM ^{15}N-cTnC were added, consecutively, aliquots of 0.5, 1.0, and 1.5 µL of 50 mM $CaCl_2$ for the first three titration points, and aliquots of 1.0, 1.0, 1.0, 1.0, 1.5, 1.5, 1.5, 1.0, 1.0, 1.0, 1.0, 2.0, 2.0, and 3.0 µL of 100 mM $CaCl_2$ were added consecutively for the next 14 individual titration points. The sample was mixed thoroughly with each addition (total of 17 additions). The total volume increase was 22.5 µL, and the change in protein concentration due to dilution was taken into account for data analysis. The change in pH from Ca^{2+} addition was negligible. Both 1D ^{1}H and 2D $\{^1H,^{15}N\}$ HSQC NMR spectra were acquired at every titration point.

$cTnI_{34–71}$ titration of ^{15}N-cTnC·3Ca^{2+}

To a NMR tube containing a 500 µL sample of 0.80 mM ^{15}N-cTnC and 5 mM $CaCl_2$ were added consecutive aliquots of 1.0 µL of 31 mM $cTnI_{34–71}$ stock solution in water for the 13 individual titration points. The sample was mixed thoroughly with each addition. The total volume increase was 13 µL, and the change in protein concentration due to dilution was taken into account for data analysis. The decrease in pH associated with $cTnI_{34–71}$ additions was adjusted by 1 M NaOH to pH 6.9 at every titration point. Both 1D ^{1}H and 2D $\{^1H,^{15}N\}$ HSQC NMR spectra were acquired at every titration point.

$cTnI_{147–163}$ titration of ^{15}N-cTnC·3Ca^{2+}·$cTnI_{34–71}$

Following titration B, the sample was filtered, and the appropriate amount of NMR buffer was added to generate a 500 µL NMR sample containing the cTnC·3Ca^{2+}·$cTnI_{34–71}$ complex. The total cTnC concentration in this sample was 0.75 mM. $cTnI_{147–163}$ peptide is highly soluble in aqueous solution but tends to form a gel at high concentrations, likely due to aggregation. Thus, no stock peptide solution was prepared; instead, solid peptide was added at every titration point (total 6 additions). The concentrations of ^{15}N-cTnC and $cTnI_{147–163}$ were determined by amino acid analysis (Smillie and Nattriss 1990) at every titration point, giving the peptide/protein ratios. The decrease in pH associated with $cTnI_{147–163}$ additions was adjusted by 1 M NaOH to pH 6.9. Both 1D ^{1}H and 2D $\{^1H,^{15}N\}$ HSQC NMR spectra were acquired at every titration point.

$cTnI_{128–147}$ titration of ^{15}N-cTnC·3Ca^{2+}

This titration was as described previously (Li et al. 2000). In the previous report, the binding affinity (K_D) was determined but the line-shape analysis was not done. The titration data were analyzed further here to determine the exchange broadening and off-rate constant (k_{off}), for the purpose of comparing with the results of $cTnI_{34–71}$ and $cTnI_{147–163}$ binding to cTnC.

NMR spectroscopy

All of the NMR spectra were obtained at 30 °C using Unity 600 MHz and Unity Inova 500 MHz spectrometers. 2D $\{^1H,^{15}N\}$ HSQC NMR spectra were acquired using the sensitivity-enhanced gradient pulse scheme developed by Lewis E. Kay and co-workers (Kay et al. 1992; Zhang et al. 1994). The ^{1}H and ^{15}N sweep widths were 7000 and 1500 Hz, respectively, on the 500 MHz spectrometer and were 8000 and 1650 Hz, respectively, on the 600 MHz spectrometer. All spectra were processed and analyzed using VNMR (Varian Associates) and NMRPipe (Delaglio et al. 1995) and referenced according to the IUPAC conventions.

Results

Ca^{2+} titration of cTnC

This study involves the use of 2D $\{^1H,^{15}N\}$ HSQC NMR spectroscopy to characterize Ca^{2+} and TnI peptide binding to the full-length cTnC. In previous studies we have demonstrated the utility of 2D $\{^1H,^{15}N\}$ HSQC NMR spectroscopy in characterizing Ca^{2+} and TnI peptide binding to the isolated N- or C-domains of sTnC or cTnC (see McKay et al. 2000 and references therein). The 2D $\{^1H,^{15}N\}$ HSQC NMR spectrum of Ca^{2+}-saturated cTnC is completely assigned (Sia et al. 1997) and used as a guide to assign the Ca^{2+}-induced spectral changes. Figure 1 depicts the Ca^{2+}-induced 2D $\{^1H,^{15}N\}$ HSQC NMR spectral changes of the backbone amide resonance in cTnC. The spectrum of apo cTnC is shown as multiple contours in Fig. 1A, in which the N-domain peaks (e.g. G70 and G42) are well dispersed, while the C-domain peaks fall within regions of ^{1}H and ^{15}N chemical shifts characterized as "random coil" by Wüthrich (1986). This suggests that the apo C-domain does not adopt a defined structure in solution, while the apo N-domain possesses a folded structure. Sites III/IV possess higher affinity than site II, so the C-domain is filled first by Ca^{2+} and this binding occurs with slow exchange kinetics on the NMR time scale. Thus, as titration progresses, the resonance peaks corresponding to a structured C-domain appear and grow (single contour peaks in Fig. 1A). This is better illustrated by the growth of D113 and D149 peaks in Fig. 2. It is interesting to notice that this growth did not stop when the $[Ca^{2+}]_{total}$/$[cTnC]_{total}$ ratio reached 2:1 and the resonance peaks corresponding to the N-domain started shifting at a

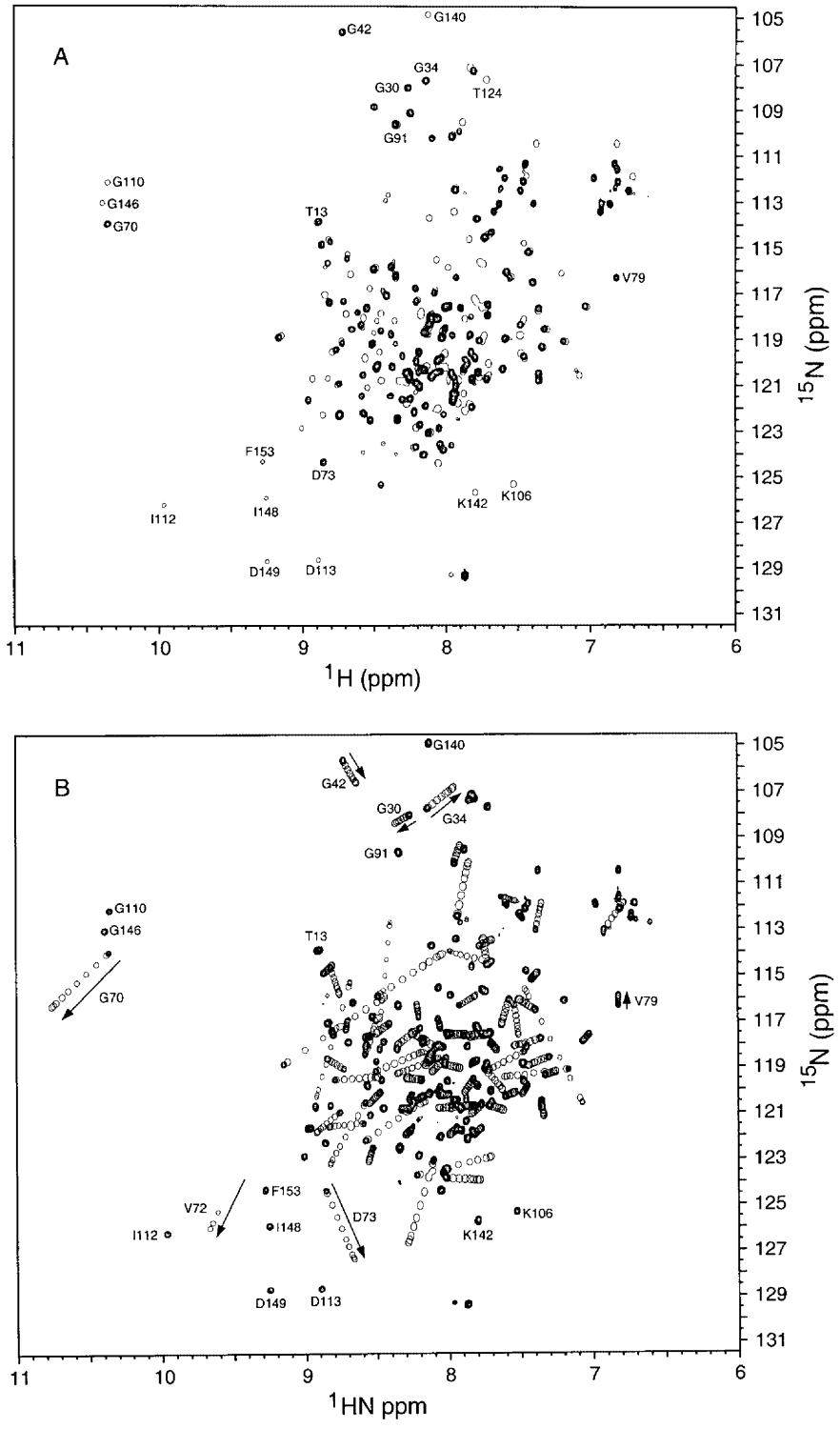

Fig. 1A, B. Titration of human intact cTnC with Ca^{2+} as monitored by 2D $\{^{1}H,^{15}N\}$ HSQC NMR spectra of the backbone amide regions of cTnC. **A** The cross peaks corresponding to apo cTnC are shown as *multiple contours*, whereas the peaks corresponding to the $[Ca^{2+}]_{total}/[cTnC]_{total}$ ratio of 1.47 are shown as *single contours*. **B** The peaks corresponding to the $[Ca^{2+}]_{total}/[cTnC]_{total}$ ratio of 1.47 are shown in *multiple contours* and the spectra representing various Ca^{2+} additions after the $[Ca^{2+}]_{total}/[cTnC]_{total}$ ratio of 1.47 are superimposed and shown as *single contours*

$[Ca^{2+}]_{total}/[cTnC]_{total}$ ratio of 1.47:1 (Fig. 1B). G70 and V72 are typical examples (Fig. 2). This indicates that site II is being partially filled before sites III/IV are completely saturated. When the intensities of D113 and D149, respectively, and the chemical shifts (both ^{1}H and ^{15}N) of G70 and V72, respectively, were measured at every titration point and the changes were averaged, normalized, and plotted as a function of the $[Ca^{2+}]_{toal}/[cTnC]_{total}$ ratio (Fig. 3), curve A corresponding to Ca^{2+} binding to sites III/IV increases rapidly and in a parallel fashion during the addition of the first and second equivalents of Ca^{2+}. During the addition of the third equivalent of Ca^{2+} it increases slowly to reach 100% occupancy. On the other hand, the gradient of curve B

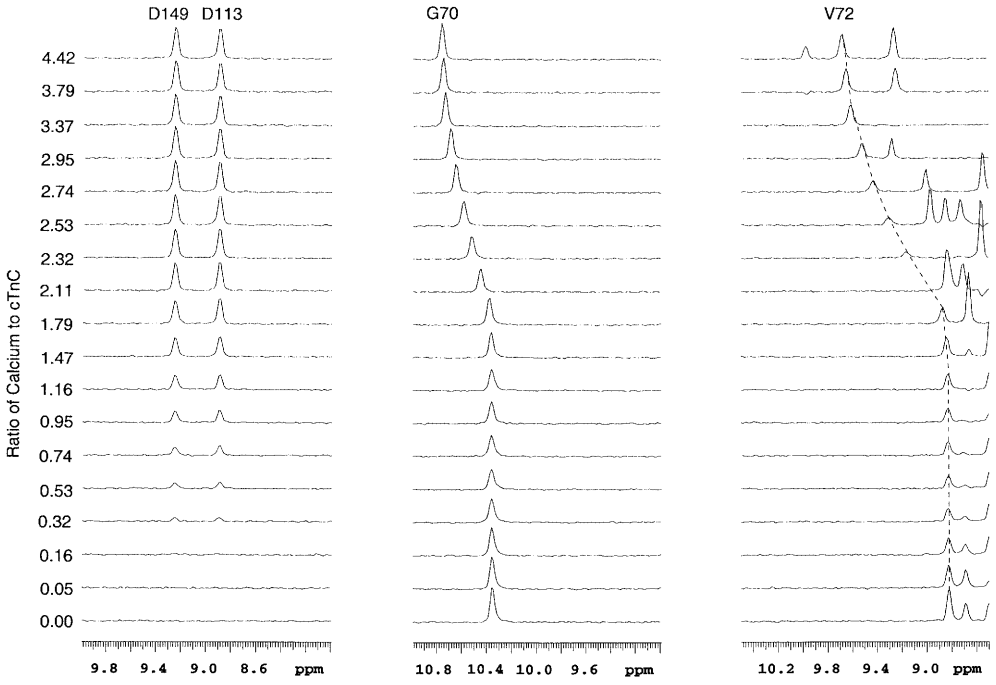

Fig. 2. Stacked plots of 1D (^{1}H dimension) traces from 2D {^{1}H,^{15}N} HSQC NMR spectral cross peaks of cTnC residues D149, D113, G70, and V72. D149 and D113 represent Ca^{2+} binding to the C-domain, while G70 and V72 represent Ca^{2+} binding to the N-domain

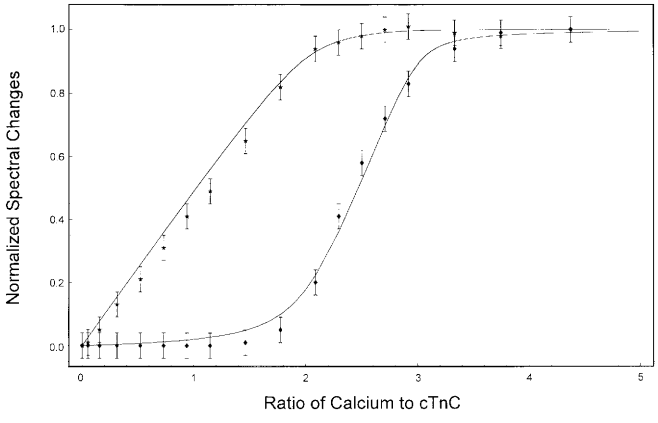

Fig. 3. Binding curves derived from the 2D {^{1}H,^{15}N} HSQC NMR spectra of cTnC upon addition of Ca^{2+}. The *upper curve* is normalized according to the average intensity changes of D149 and D113, representing Ca^{2+} binding to the C-domain, while the *lower curve* is normalized according to averaged chemical shift changes of G70 and V72, representing Ca^{2+} binding to the N-domain. The best-fit curves to the data are shown by *solid lines*. The curve fitting procedures are as described in Results

(Fig. 3), corresponding to Ca^{2+} binding to site II, increases slowly during addition of the first two equivalents of Ca^{2+} and increases rapidly in the region between two and three equivalents to reach 100% occupancy. The curves indicate that all three sites have some degree of occupancy from the first addition of Ca^{2+} and that the occupancy of all three sites is essentially completed when three equivalents of Ca^{2+} have been added.

Assuming sites III and IV in the C-domain are independent and equal, which is not distinguished from 100% positive cooperativity, and site II is independent of sites III and IV, and assuming each of the three sites (II, III, IV) binds Ca^{2+} in a 1:1 stoichiometry, the spectral changes as a function of $[Ca^{2+}]_{total}/[cTnC]_{total}$ were fit to the equations:

$$\text{Site III} + Ca^{2+} \rightleftharpoons \text{Site III}.Ca^{2+} \quad (1)$$

$$\text{Site IV} + Ca^{2+} \rightleftharpoons \text{Site IV}.Ca^{2+} \quad (2)$$

$$\text{Site II} + Ca^{2+} \rightleftharpoons \text{Site II}.Ca^{2+} \quad (3)$$

and yielded macroscopic dissociation constants of $K_{D(III,IV)} \approx 0.2$ μM for sites III and IV and $K_{D(II)} \approx 20$ μM for site II, respectively. This fitting also permits the calculation of a site III and IV occupancy of ~90% and a site II occupancy of ~20% at 2 equivalents of Ca^{2+} (the curve fitting script used is available upon request from brian.sykes@ualberta.ca). These results are consistent with the consensus results that the C-domain sites III/IV have ~100-fold higher Ca^{2+} binding affinity than the N-domain site II. However, the determined site II dissociation constant of $K_D \approx 20$ μM is approximately 10 times weaker than that for native cTnC reported previously (Hannon et al. 1992; Hazard et al. 1998; Holroyde et al. 1980; Johnson et al. 1980). This discrepancy is probably due to the fact that the previous reported affinities were measured at lower temperatures (e.g. 4 °C) and it is likely that site II binds Ca^{2+} tighter at lower temperatures than at 30 °C. Ca^{2+} titration of cTnC at lower temperatures (e.g. 4 °C) by the use of 2D {^{1}H,^{15}N} HSQC NMR spectroscopy would provide insight into this matter, a project currently in progress in our laboratory. Somewhat surprisingly, this affinity is also ~10 times weaker than what we have observed in the Ca^{2+}

titration of cNTnC ($K_D = 2.6$ μM) (Li et al. 1997). It seems that the presence of the C-terminal domain somehow reduced the affinity of Ca^{2+} for the N-domain of cTnC. At present, there is no compelling data for rationalization.

In addition to the Ca^{2+}-induced intensity and chemical shift changes, individual cross peaks in the 2D $\{^1H,^{15}N\}$ HSQC NMR spectra during Ca^{2+} titration display differential broadening, especially those in the N-domain, indicating exchange broadening. Typical examples are G70 and V72, as shown in Fig. 2. The NMR spectral changes can occur in fast, intermediate, and/or slow exchange limit on the NMR time scale, depending on the size of the Ca^{2+}-induced resonance shift (Li et al. 1995). In the intermediate to fast exchange limit, the effect of chemical exchange on linewidth is dependent on the chemical shift differences between free and bound species:

$$\Delta\nu_{ex} = P_f P_b \tau_{ex} (\Delta\delta_i)^2 \quad (4)$$

where $\Delta\nu_{ex}$ is the observed line width, P_f and P_b are the populations of free and bound cTnC, and τ_{ex} is the exchange lifetime defined as $(\tau_f\tau_b)/(\tau_f + \tau_b)$. Previously, we have used the linewidth simulation to analyze the behavior of the 2D $\{^1H,^{15}N\}$ HSQC NMR spectra taken during titrations of sTnC with sTnI peptides (McKay et al. 1997, 1999). Here we use the same approach to analyze the 2D $\{^1H,^{15}N\}$ HSQC NMR spectral changes induced by Ca^{2+} binding to the N-domain of cTnC. One-dimensional traces in the ^1H dimension through the cross peaks of residues G42, D73, G70, and V72 are shown in Fig. 4 to demonstrate the effect of exchange at various titration points during the addition of Ca^{2+}. For G42, where the $\Delta\delta = 43$ Hz, the line shape only slightly broadens during the titration. On the other hand, V72, which has $\Delta\delta = 424$ Hz, broadens substantially during the titration and then sharpens dramatically at the end. The $\Delta\delta$ values for D73 and G70 are 92 Hz and 201 Hz, respectively, and the line broadening fell between G42 and V72. The line-shape changes for these four residues were simulated to obtain the site II Ca^{2+} off-rate constant k_{off}. The line widths of the free ($\Delta\nu_f$) and bound ($\Delta\nu_b$) species and the starting (δ_f) and final (δ_b) resonance positions for those four residues are listed in the legend of Fig. 4. The simulations were done using the experimentally derived values for $\Delta\nu_f$, $\Delta\nu_b$, δ_f, δ_b, and $K_{D(II)} = 20$ μM and $K_{D(III/IV)} = 0.2$ μM and adjusting k_{off}. A k_{off} of 5000 s^{-1} provides the closest fit to the experimental data for all four residues (Fig. 4). Since the simulation program does not take into account the relaxation in both ^1H and ^{15}N dimensions during the 2D $\{^1H,^{15}N\}$ HSQC pulse sequence, which will lead to lower intensities in the middle of the titration when the line broadening is the largest, differential intensities of the cross peaks between the simulated and experimental spectra are observed (X. Wang, M.X. Li, B.D. Sykes, unpublished data). The most obvious is with V72 (Fig. 4). The site II Ca^{2+} off-rate of 5000 s^{-1} at 30 °C had not been measured previously because this rate is too fast to be measured by fluorescence stopped-flow experiments. Using the relationship $K_D = k_{off}/k_{on}$, the calculated k_{on} is 2.5×10^8 M^{-1} s^{-1}, indicating that Ca^{2+} binding to site II is diffusion controlled at 30 °C.

Fig. 4. 1D (^1H dimension) traces taken through the 2D $\{^1H,^{15}N\}$ HSQC NMR spectral cross peaks of G42, D73, G70, and V72 during Ca^{2+} titration are shown in the *lower panels*. While the peaks of G42 and D73 shift *from left to right*, those of G70 and V72 shift *from right to left*. The *upper panels* are computer simulations using $K_{D(III/IV)} = 0.2$ μM, $K_{D(II)} = 20$ μM, and $k_{off} = 5000$ s^{-1}. The line widths of the free ($\Delta\nu_f$) and the bound ($\Delta\nu_b$) species and the starting (δ_f) and the final (δ_b) resonance positions for those four residues are as follows: G42, $\Delta\nu_f = 19$, $\Delta\nu_b = 21$, $\delta_f = 4358$, and $\delta_b = 4315$ Hz; D73, $\Delta\nu_f = 21$, $\Delta\nu_b = 23$, $\delta_f = 4424$, and $\delta_b = 4332$ Hz; G70, $\Delta\nu_f = 21$, $\Delta\nu_b = 21$, $\delta_f = 5178$, and $\delta_b = 5379$ Hz; V72, $\Delta\nu_f = 22$, $\Delta\nu_b = 23$, $\delta_f = 4409$, and $\delta_b = 4833$ Hz

$cTnI_{34-71}$ titration of $cTnC{\cdot}3Ca^{2+}$

Previously, we have shown that $cTnI_{34-71}$ binds $cCTnC{\cdot}2Ca^{2+}$ in a 1:1 stoichiometry to form a stable $cCTnC{\cdot}2Ca^{2+}{\cdot}cTnI_{34-71}$ complex ($K_D = 1$ μM) and the interaction of $cTnI_{34-71}$ with $cCTnC{\cdot}2Ca^{2+}$ occurs with slow exchange kinetics on the NMR time scale (Wang et al. 2001). Here we show a similar binding behavior of $cTnI_{34-71}$ for $cTnC{\cdot}3Ca^{2+}$, indicating that the interaction of this region of cTnI binds specifically to the C-domain of $cTnC{\cdot}3Ca^{2+}$ regardless of the presence of

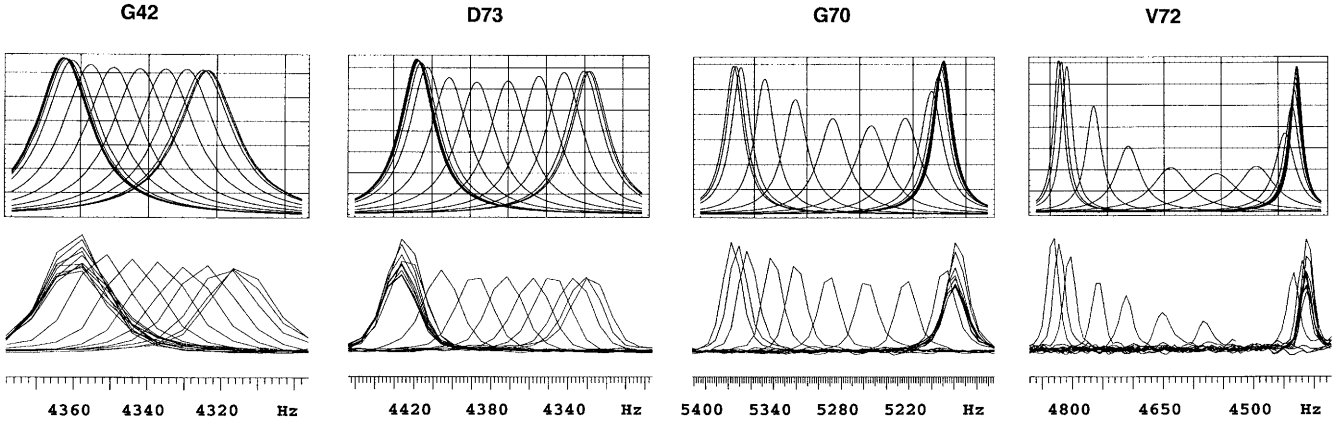

the N-domain. Figure 5A shows a superimposition of the 2D $\{^1H,^{15}N\}$ HSQC NMR spectra of cTnC·$3Ca^{2+}$ and the cTnC·$3Ca^{2+}$·$cTnI_{34–71}$ complex. As the titration progresses, the resonance peaks corresponding to cTnC·$3Ca^{2+}$ becomes less intense while those corresponding to the cTnC·$3Ca^{2+}$·$cTnI_{34–71}$ complex grow. Only the C-domain residues are affected (Fig. 5A). For example, G110 and G146 shift to new positions, while G70 peak does not move at all. When the peptide to protein ratio reaches 1:1, all cross peaks corresponding to the C-domain of cTnC·$3Ca^{2+}$ have completely disappeared, while those corresponding to the complex attain maximum intensity. This phenomenon is more clearly illustrated in Fig. 6A. The intensity changes as a function of peptide to protein ratios were fit to the equation:

$$cTnC.3Ca^{2+} + cTnI_{34–71} \rightleftharpoons cTnC.3Ca^{2+}.cTnI_{34–71} \quad (5)$$

and yielded a dissociation constant (K_D) of 1 μM, agreeing with the affinity of $cTnI_{34–71}$ for cCTnC·$2Ca^{2+}$ (Wang et al. 2001) and that of $sTnI_{1–40}$ for sCTnC·$2Ca^{2+}$ (Mercier et al. 2000). The line shapes of

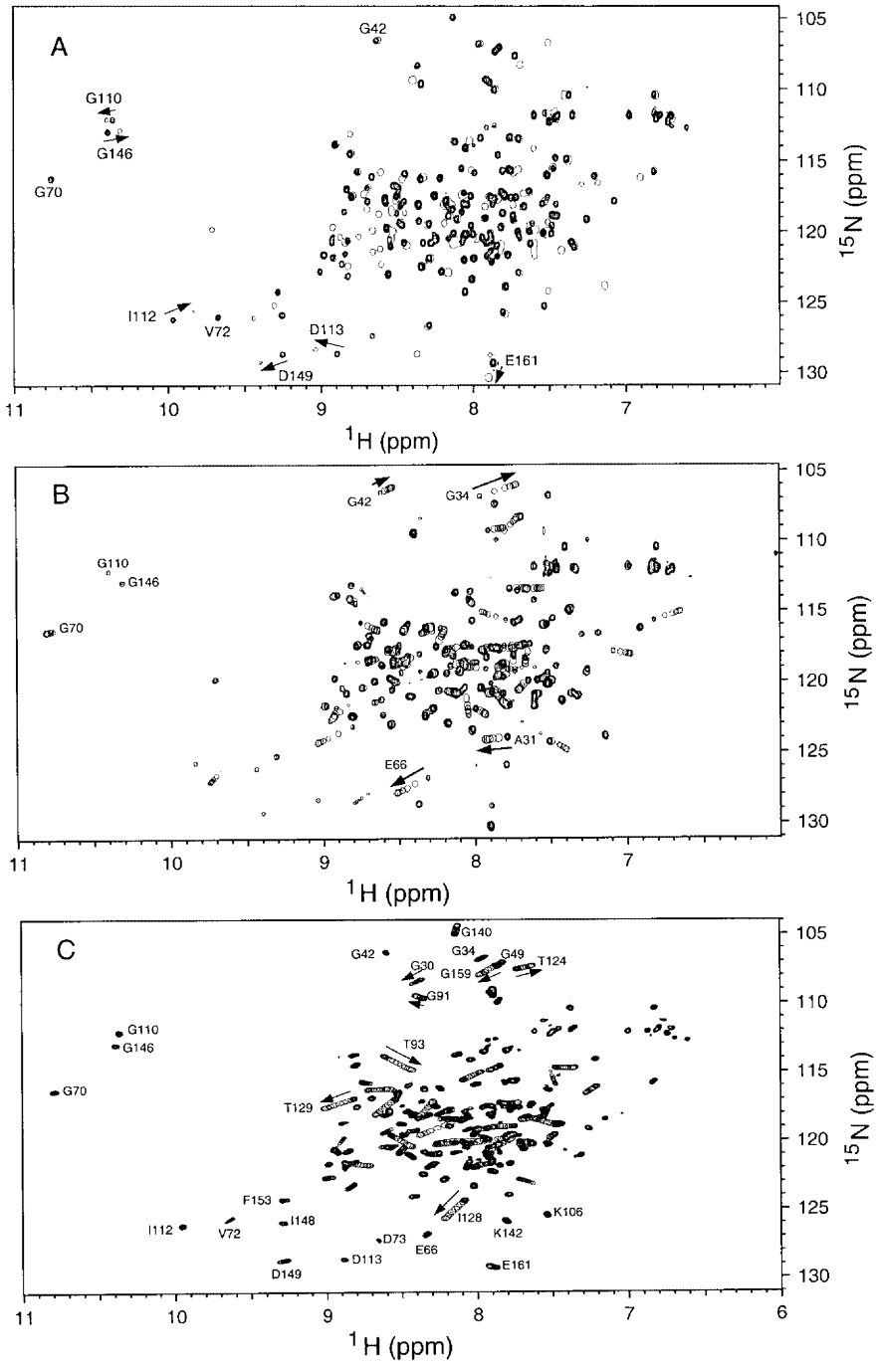

Fig. 5. Titration of **A** cTnC·$3Ca^{2+}$ with $cTnI_{34–71}$, **B** cTnC·$3Ca^{2+}$·$cTnI_{34–71}$ with $cTnI_{147–163}$, and **C** cTnC·$3Ca^{2+}$ with $cTnI_{128–147}$ as monitored 2D $\{^1H,^{15}N\}$ HSQC NMR spectra from the backbone amide regions of cTnC. In all three cases the binding stoichiometry is 1:1. **A** The cross peaks corresponding to cTnC·$3Ca^{2+}$ are shown as *multiple contours*, whereas those corresponding to cTnC·$3Ca^{2+}$·$cTnI_{34–71}$ are shown as *single contours*. **B** The cross peaks corresponding to cTnC·$3Ca^{2+}$·$cTnI_{34–71}$ are shown as *multiple contours* and the spectra representing various $cTnI_{147–163}$ additions are superimposed and shown as *single contours*. **C** The cross peaks corresponding to cTnC·$3Ca^{2+}$ are shown as *multiple contours* and the spectra representing various $cTnI_{128–147}$ additions are superimposed and shown as *single contours*

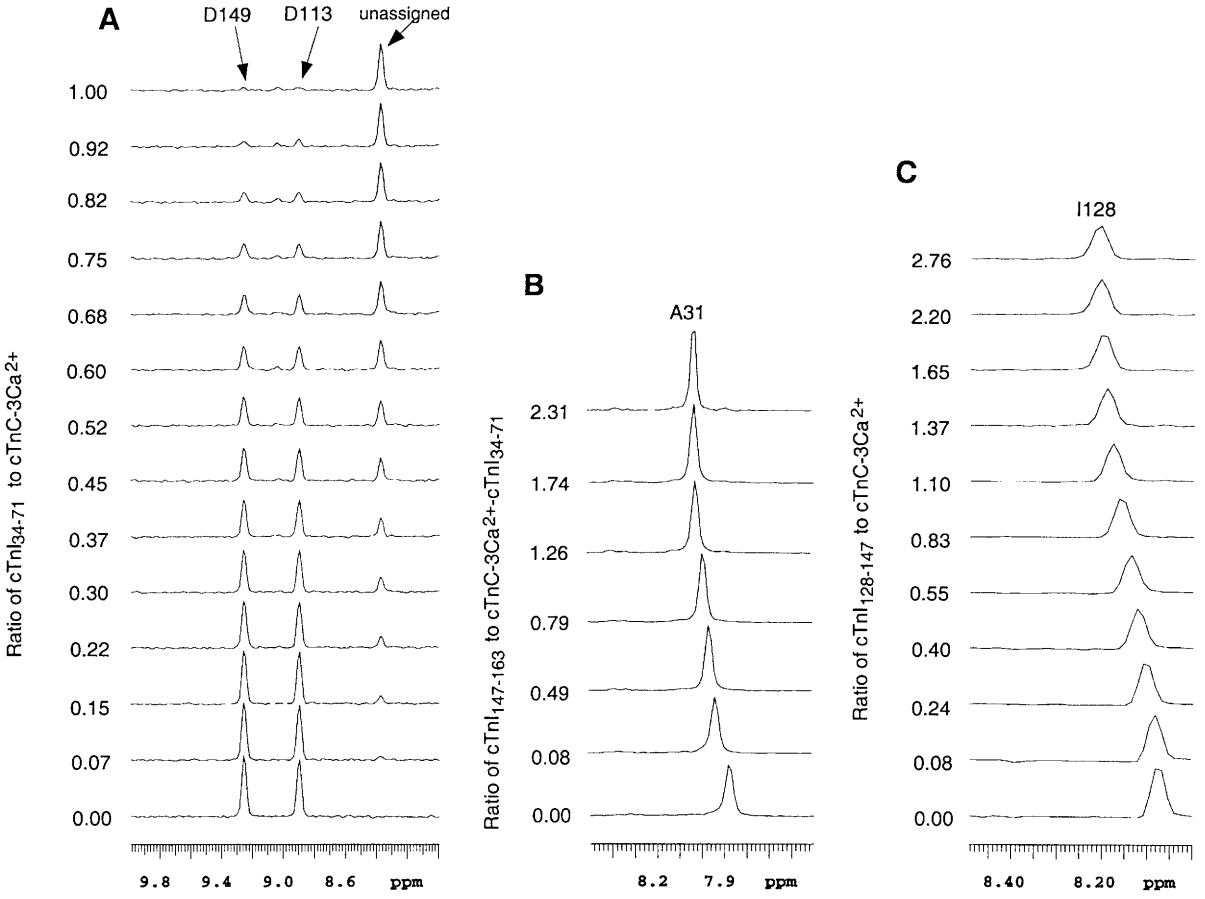

Fig. 6. Stacked plots of 1D (^{1}H dimension) traces from 2D $\{^1H,^{15}N\}$ HSQC NMR spectral cross peaks of cTnC residues D113 and D149, A31, and I128, respectively representing **A** $cTnI_{34–71}$ binding to $cTnC{\cdot}3Ca^{2+}$, **B** $cTnI_{147–163}$ binding to $cTnC{\cdot}3Ca^{2+}{\cdot}cTnI_{34–71}$, and **C** $cTnI_{128–147}$ binding to $cTnC{\cdot}3Ca^{2+}$

G110 were simulated using experimentally derived values of $\Delta\nu_f = 20$ Hz, $\Delta\nu_b = 24$ Hz, $\delta_f = 6215$ Hz, $\delta_b = 6329$ Hz, $\Delta\delta = 114$ Hz, and $K_D = 1$ μM and adjusting k_{off}. A k_{off} value of 5 s^{-1} provides the closest fit to the experimental data (Fig. 7A). This indicates that the dissociation of this region of cTnI may be too slow to participate in muscle regulation.

$cTnI_{147–163}$ titration of $cTnC{\cdot}3Ca^{2+}{\cdot}cTnI_{34–71}$

Previously, we have titrated $cTnI_{147–163}$ to $cNTnC{\cdot}Ca^{2+}$ and determined a binding affinity (K_D) of 154 ± 10 μM (Li et al. 1999). In this study, we show the titration of this peptide to $cTnC{\cdot}3Ca^{2+}{\cdot}cTnI_{34–71}$. In this complex the C-domain hydrophobic pocket is occupied by $cTnI_{34–71}$, which binds tightly ($K_D = 1$ μM). Figure 5B shows the superimposition of the 2D $\{^1H,^{15}N\}$ HSQC NMR spectra of $cTnC{\cdot}3Ca^{2+}{\cdot}cTnI_{34–71}$ titrated by $cTnI_{147–163}$. Similar to $cTnI_{147–163}$ binding to $cNTnC{\cdot}Ca^{2+}$, this reaction occurs with fast exchange kinetics on the NMR time scale. Figure 6B shows the shifts of the A31 resonance and the chemical shift changes of A31 as a function of peptide to protein ratios were fit to the equation:

$$cTnC.3Ca^{2+} + cTnI_{34–71} + cTNI_{147–163} \rightleftarrows cTnC.3Ca^{2+}.cTnI_{34–71}.cTnI_{147–163} \quad (6)$$

and yielded a K_D of 150 ± 10 μM. Within experimental error, this affinity agrees with that of $cTnI_{147–163}$ for $cNTnC{\cdot}Ca^{2+}$, indicating that the affinity of this peptide for the N-domain of cTnC is independent of the presence of the C-domain. The line shapes of A31 were simulated using experimentally derived values of $\Delta\nu_f = 21$ Hz, $\Delta\nu_b = 16$ Hz, $\delta_f = 3938$ Hz, $\delta_b = 4012$ Hz, $\Delta\delta = 74$ Hz, and $K_D = 150$ μM and adjusting k_{off}. A k_{off} of 5000 s^{-1} provides the closest fit to the experimental data (Fig. 7B). This indicates that the dissociation rate of this region of cTnI from cTnC is in the same order of Ca^{2+} dissociation from site II and is fast enough to regulate muscle contraction.

$cTnI_{128–147}$ titration of $cTnC{\cdot}3Ca^{2+}$

This titration was done in a previous study and we have reported the binding affinity of 78 ± 10 μM (Li et al. 2000), but the line-shape analysis was not done. For the purpose of comparing with the binding of the other two

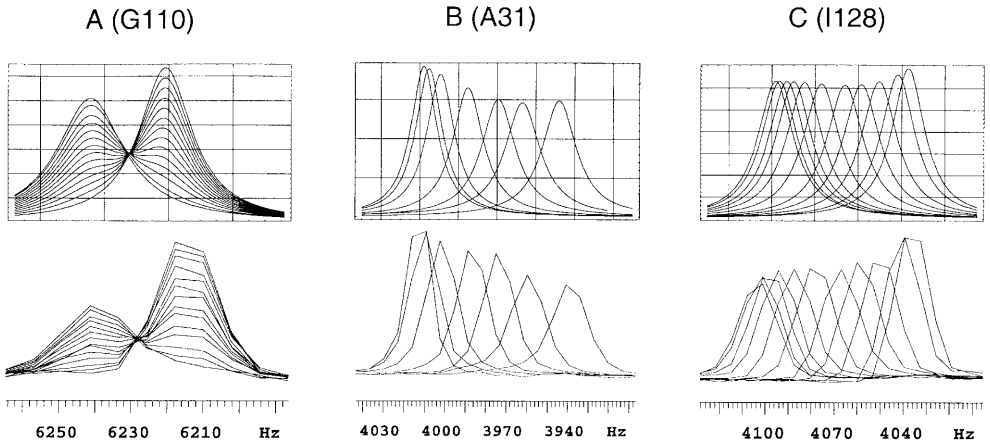

Fig. 7. 1D (^{1}H dimension) NMR spectral traces taken through the 2D $\{^1H,^{15}N\}$ HSQC NMR spectral cross peaks of G110 in the titration of cTnC·3Ca^{2+} with cTnI$_{34-71}$ (**A**), A31 in the titration of cTnC·3Ca^{2+}·cTnI$_{34-71}$ with cTnI$_{147-163}$ (**B**), and I128 in the titration of cTnC·3Ca^{2+} with cTnI$_{128-147}$ (**C**), respectively, are shown in the *lower panels*. All three residues shift *from left to right*. The *upper panels* are computer simulations using $K_D = 1$ μM and $k_{off} = 5$ s^{-1} for **A**, $K_D = 150$ μM and $k_{off} = 5000$ s^{-1} for **B**, and $K_D = 78$ μM and $k_{off} = 5000$ s^{-1} for **C**, respectively

regions of cTnI to cTnC, the titration plot of cTnC·3Ca^{2+} with cTnI$_{128-147}$ is shown in Fig. 5C. Figure 6C shows the shifts of the I128 resonance. The chemical shift changes of I128 as a function of peptide to protein ratios were fit to the equation:

$$cTnC.3Ca^{2+} + cTnI_{128-147} \rightleftarrows cTnC.3Ca^{2+}.cTnI_{128-147} \quad (7)$$

and yielded a K_D of 78 ± 10 μM. The line shapes of the I128 resonances were simulated using experimentally derived values of $\Delta\nu_f = 18$ Hz, $\Delta\nu_b = 20$ Hz, $\delta_f = 4037$ Hz, $\delta_b = 4103$ Hz, $\Delta\delta = 66$ Hz, and $K_D = 78$ μM and adjusting k_{off}. A k_{off} of 5000 s^{-1} provides the closest fit to the experimental data (Fig. 7C). This indicates that the dissociation rate of this region of cTnI from cTnC is in the same order of Ca^{2+} dissociation from site II and is fast enough to regulate muscle contraction.

Discussion

The key events in regulating skeletal and cardiac muscle contraction involve Ca^{2+} binding and release from TnC, the accompanied structural changes, and the subsequent TnC-TnI interactions. Although the sequence of events involved in initiating skeletal and cardiac muscle contraction are very similar, the kinetics and thermodynamics of these events must differ for the two systems to account for the different physiological behavior of the two muscle types. The goal of this study is to characterize the kinetics of Ca^{2+} binding to intact human cTnC and of three cTnI peptides binding to the Ca^{2+}-saturated cTnC by the means of 2D $\{^1H,^{15}N\}$ HSQC NMR spectroscopy at 30 °C, a temperature close to that of human heart (~37 °C). The kinetics of these events are reflected in the Ca^{2+}- and peptide-induced NMR spectral intensity, chemical shift, and line-shape changes of cTnC. Analysis of the NMR spectral changes allow us to determine the dissociation (K_D) and off-rate (k_{off}) constants and to derive the association rate (k_{on}) constants using the relationship $K_D = k_{off}/k_{on}$.

We first examined Ca^{2+} binding to both classes of sites in intact human cTnC. The results show that sites III and IV exhibit 100-fold higher Ca^{2+} affinity than site II ($K_{D(III,IV)} \approx 0.2$ μM, $K_{D(II)} \approx 20$ μM), but that site II is partially occupied before sites III and IV are saturated. The addition of the first two equivalents of Ca^{2+} saturates ~90% of sites III and IV and ~20% of site II and three equivalents saturate all three sites completely. This suggests that the Ca^{2+} occupancy of all three sites may contribute to the Ca^{2+}-dependent regulation in muscle contraction. A similar phenomenon in Ca^{2+} binding to CaM has been reported (Biekofsky et al. 1998), demonstrating that the addition of two equivalents of Ca^{2+} saturates 15–35% of the N-domain sites (I/II) and 85–55% of the C-domain sites (III/IV). This is not surprising, since both classes of binding sites in CaM play regulatory roles (for a review see Crivici and Ikura 1995). For cTnC or sTnC, such a behavior had not been reported previously. Biekofsky et al. (1998) also reported line broadening of the N-domain resonances (e.g. I27 and I63) during Ca^{2+} binding to the C-domain and interpreted it as due to the partial occupancy of sites I/II in CaM. In this work, we also observed line broadening of the N-domain resonances (e.g. G70 and V72, Fig. 2) during Ca^{2+} binding to the C-domain of cTnC. V72 is the residue equivalent to I63 in CaM. Clearly, this is the result of the partial occupancy of site II before the $[Ca^{2+}]_{total}/[cTnC]_{total}$ ratio reaches 2. Thus, no domain-domain interactions need be introduced to understand the NMR spectral changes occurring during Ca^{2+} titration of cTnC.

A second major finding from this study is that a much higher site II Ca^{2+} dissociation rate ($k_{off} = 5000$ s^{-1}, 30 °C) was observed as compared to previous published results. Such a rapid off-rate had not previously been

measured. A number of studies have been performed on the kinetics of Ca^{2+} binding to sTnC or cTnC, isolated or in the troponin complex, and the experiments involve the use of proteins with mutated or attached fluorescent reporter groups. In sTnC, Ca^{2+} binding to sites I/II appears to be diffusion limited ($k_{on} \approx 10^8$ M^{-1} s^{-1}) with a Ca^{2+} dissociation rate (k_{off}) of ~400–500 s^{-1} and the conformational change occurs almost simultaneously with the Ca^{2+} association/dissociation (Johnson et al. 1994; Rosenfeld and Taylor 1985a, 1985b). In cTnC, Ca^{2+} binding to site II is also diffusion limited ($k_{on} \approx 10^8$ M^{-1} s^{-1}, $k_{off} \approx$ 500–800 s^{-1}), but the conformational change was found to be significantly slower than the Ca^{2+} on- and off-rates (Dong et al. 1996, 1997; Hazard et al. 1998). These reported on- and off-rates may not, however, represent the time scales of the molecular events that would occur at physiological temperature (e.g. 37 °C in human heart), since most of these experiments were performed at 4 °C because Ca^{2+} kinetics become too fast to be measured by stopped-flow methods at temperatures higher than 4 °C (Hazard et al. 1998). Moreover, it is well known that both the time to peak tension after excitation and the relaxation time can vary widely with temperature, and are species-dependent. Knowing the dissociation constant $K_{D(II)} = 20$ μM and off-rate constant $k_{off} = 5000$ s^{-1}, the calculated on-rate of Ca^{2+} ($K_{D(II)} = k_{off}/k_{on}$) for site II is 2.5×10^8 M^{-1} s^{-1}, indicating that Ca^{2+} binding to site II of cTnC is diffusion-controlled. Hence, at a temperature (30 °C) close to the physiological level, Ca^{2+} association and dissociation from site II is rapid enough to account for the speed of cardiac muscle contraction and relaxation, which occur on the time scale of milliseconds (Mason 1983).

The rapid rate of the rise of the tension necessitates a rapid binding of Ca^{2+} to the Ca^{2+}-specific regulatory site II of cTnC as well as a rapid propagation of these Ca^{2+}-induced conformational changes to other components of the thin filaments, such as cTnI. Limited information is available on the kinetics of sTnC-sTnI or cTnC-cTnI interactions. In a previous study, we initiated the kinetic analysis of sTnC-sTnI interaction by studying the binding of the $sTnI_{115–131}$ peptide to $sNTnC{\cdot}2Ca^{2+}$ (McKay et al. 1997). In the present work, we have determined the off-rate constants for the binding of three cTnI peptides to cTnC: these are 5 s^{-1} for $cTnI_{34–71}$, 5000 s^{-1} for $cTnI_{128–147}$, and 5000 s^{-1} for $cTnI_{147–163}$, respectively. Thus, it appears that the k_{off} values for the binding of $cTnI_{128–147}$ and $cTnI_{147–163}$ to cTnC are in the same order as the k_{off} for the binding of Ca^{2+} to site II of cTnC, and these events are fast enough to be kinetically competent for muscle contraction, while that of $cTnI_{34–71}$ may be too slow for this process. These three regions of cTnI have been identified by many biophysical and biological studies to be responsible for interacting with cTnC. In the antiparallel arrangement of cTnC-cTnI interaction (Farah and Reinach 1995; Krudy et al. 1994), $cTnI_{34–71}$, corresponding to $sTnI_{1–40}$, binds tightly to the Ca^{2+}-saturated C-domain of cTnC and the binding site was identified to be in the hydrophobic pocket of the C-domain (Gasmi-Seabrook et al. 1999). This region of cTnI presumably adopts an α-helical conformation similar to that of $sTnI_{1–47}$ observed in the X-ray structure of the $sTnC{\cdot}2Ca^{2+}{\cdot}sTnI_{1–47}$ complex (Vassylyev et al. 1998). The inhibitory domain of cTnI ($cTnI_{128–147}$) binds to the central helix area toward the C-domain of cTnC and this binding constitutes a major switch between muscle contraction and relaxation (Van Eyk and Hodges 1988); this switch is also modulated by the interaction of the C-terminal region of cTnI and cTnC (Ramos 1999; Rarick et al. 1997). The residues (~147–163) immediately following the inhibitory region bind to the hydrophobic pocket of the N-domain of cTnC. In the NMR structure of $cTnI_{147–163}$ in complex with $cNTnC{\cdot}Ca^{2+}$, $cTnI_{147–163}$ forms an α-helix and interacts with the hydrophobic surface of the N-domain, stabilizing its open conformation (Li et al. 1999). Two models of sTnC-sTnI interactions have been proposed to rationalize the functional roles of these three regions of TnI. One proposes that the N-terminal and the inhibitory regions share overlapping binding sites on the C-domain of sTnC, which are alternatively occupied by either one or the other depending on the interactions between the N-domain of TnC and the C-domain of TnI (Tripet et al. 1997). Another proposes that the N-terminal region of TnI always binds to the C-domain of TnC regardless of the Ca^{2+}-dependent interaction between the N-domain of TnC and the C-domain of TnI, while the inhibitory region interacts with the central helix area (Luo et al. 2000; Tung et al. 2000). Clearly, our results are in line with the second model, which implies a structural role for the $cTnI_{34–71}$ region but functional roles for both the $cTnI_{128–147}$ and $cTnI_{147–163}$ regions.

Acknowledgements We are indebted to Mr. Pascal Mercier for help with the Mathematica Scripts used to simulate the binding affinities and off-rate constants. We thank Mr. Gerry McQuaid for NMR spectrometer maintenance and Mr. David Corson for expression and purification of the cTnC proteins. This work was supported by the Canadian Institutes of Health Research (CIHR) and the Heart and Stroke Foundation of Canada.

References

Biekofsky RR, Martin SR, Browne JP, Bayley PM, Feeney J (1998) Ca^{2+} coordination to backbone carbonyl oxygen atoms in calmodulin and other EF-hand proteins: ^{15}N chemical shifts as probes for monitoring individual-site Ca^{2+} coordination. Biochemistry 37:7617–7629

Crivici A, Ikura M (1995) Molecular and structural basis of target recognition by calmodulin. Annu Rev Biophys Biomol Struct 24:85–116

Delaglio F, Grzesiek S, Vuister GW, Zhu G, Pfeifer J, Bax A (1995) NMRPipe: a multidimensional spectral processing system based on UNIX pipes. J Biomol NMR 6:277–293

Dong W, Rosenfeld SS, Wang CK, Gordon AM, Cheung HC (1996) Kinetic studies of calcium binding to the regulatory site of troponin C from cardiac muscle. J Biol Chem 271:688–694

Dong WJ, Wang CK, Gordon AM, Rosenfeld SS, Cheung HC (1997) A kinetic model for the binding of Ca^{2+} to the regula-

tory site of troponin from cardiac muscle. J Biol Chem 272:19229–19235
Farah CS, Reinach FC (1995) The troponin complex and regulation of muscle contraction. FASEB J 9:755–767
Gagné SM, Tsuda S, Li MX, Smillie LB, Sykes BD (1995) Structures of the troponin C regulatory domains in the apo and calcium-saturated states. Nat Struct Biol 2:784–789
Gagné SM, Li MX, McKay RT, Sykes BD (1998) The NMR angle on troponin C. Biochem Cell Biol 76:302–312
Gasmi-Seabrook GM, Howarth JW, Finley N, Abusamhadneh E, Gaponenko V, Brito RM, Solaro RJ, Rosevear PR (1999) Solution structures of the C-terminal domain of cardiac troponin C free and bound to the N-terminal domain of cardiac troponin I. Biochemistry 38:8313–8322
Geeves MA, Holmes KC (1999) Structural mechanism of muscle contraction. Annu Rev Biochem 68:687–728
Gordon AM, Homsher E, Regnier M (2000) Regulation of contraction in striated muscle. Physiol Rev 80:853–924
Hannon JD, Martyn DA, Gordon AM (1992) Effects of cycling and rigor crossbridges on the conformation of cardiac troponin C. Circ Res 71:984–991
Hazard AL, Kohout SC, Stricker NL, Putkey JA, Falke JJ (1998) The kinetic cycle of cardiac troponin C: calcium binding and dissociation at site II trigger slow conformational rearrangements. Protein Sci 7:2451–2459
Herzberg O, Moult J, James MNG (1986) A model for the Ca^{2+}-induced conformational transition of troponin C. J Biol Chem 261:2638–2644
Holroyde MJ, Robertson SP, Johnson JD, Solaro RJ, Potter JD (1980) The calcium and magnesium binding sites on cardiac troponin and their role in the regulation of myofibrillar adenosine triphosphatase. J Biol Chem 255:11688–11693
Johnson JD, Collins JH, Robertson SP, Potter JD (1980) A fluorescent probe study of Ca^{2+} binding to the Ca^{2+}-specific sites of cardiac troponin and troponin C. J Biol Chem 255:9635–9640
Johnson JD, Nakkula RJ, Vasulka C, Smillie LB (1994) Modulation of Ca^{2+} exchange with the Ca^{2+}-specific regulatory sites of troponin C. J Biol Chem 269:8919–8923
Kay LE, Keifer P, Saarinen T (1992) Pure absorption gradient enhanced heteronuclear single quantum correlation spectroscopy with improved sensitivity. J Am Chem Soc 114:10663–10665
Krudy GA, Kleerekoper Q, Guo X, Howarth JW, Solaro RJ, Rosevear PR (1994) NMR studies delineating spatial relationships within the cardiac troponin I-troponin C complex. J Biol Chem 269:23731–23735
Li MX, Gagné SM, Tsuda S, Kay CM, Smillie LB, Sykes BD (1995) Calcium binding to the regulatory N-domain of skeletal muscle troponin C occurs in a stepwise manner. Biochemistry 34:8330–8340
Li MX, Gagné SM, Spyracopoulos L, Kloks CPAM, Audette G, Chandra M, Solaro RJ, Smillie LB, Sykes BD (1997) NMR studies of Ca^{2+}-binding to the regulatory domains of cardiac and E41A skeletal muscle troponin C reveal importance of site I to energetics of the induced structural changes. Biochemistry 36:12519–12525
Li MX, Spyracopoulos L, Sykes BD (1999) Binding of cardiac troponin-$I_{147–163}$ induces a structural opening in human cardiac troponin-C. Biochemistry 38:8289–8298
Li MX, Spyracopoulos L, Beier N, Putkey JA, Sykes BD (2000) Interaction of cardiac troponin C with Ca^{2+} sensitizer EMD 57033 and cardiac troponin I inhibitory peptide. Biochemistry 39:8782–8790
Luo Y, Wu JL, Li B, Langsetmo K, Gergely J, Tao T (2000) Photocrosslinking of benzophenone-labeled single cysteine troponin I mutants to other thin filament proteins. J Mol Biol 296:899–910
Mason EB (1983) Human physiology, Benjamin/Cummings, Menlo Park, Calif
McKay RT, Tripet BP, Hodges RS, Sykes BD (1997) Interaction of the second binding region of troponin I with the regulatory domain of skeletal muscle troponin-C as determined by NMR spectroscopy. J Biol Chem 272:28494–28500
McKay RT, Tripet BP, Pearlstone JR, Smillie LB, Sykes BD (1999) Defining the region of troponin-I that binds to troponin-C. Biochemistry 38:5478–5489
McKay RT, Saltibus LF, Li MX, Sykes BD (2000) Energetics of the induced structural change in a Ca^{2+} regulatory protein: Ca^{2+} and troponin I peptide binding to the E41A mutant of the N-domain of skeletal troponin C. Biochemistry 39:12731–12738
Mercier P, Li MX, Sykes BD (2000) Role of the structural domain of troponin C in muscle regulation: NMR studies of Ca^{2+} binding and subsequent interactions with regions 1–40 and 96–115 of troponin I. Biochemistry 39:2902–2911
Pearlstone JR, Chandra M, Sorenson MM, Smillie LB (2000) Biological function and site II Ca^{2+}-induced opening of the regulatory domain of skeletal troponin C are impaired by invariant site I or II Glu mutations. J Biol Chem 275:35106–35115
Putkey JA, Sweeney HL, Campbell ST (1989) Site-directed mutation of the trigger calcium-binding sites in cardiac troponin C. J Biol Chem 264:12370–12378
Ramos CH (1999) Mapping subdomains in the C-terminal region of troponin I involved in its binding to troponin C and to thin filament. J Biol Chem 274:18189–18195
Rarick HM, Tu XH, Solaro RJ, Martin AF (1997) The C terminus of cardiac troponin I is essential for full inhibitory activity and Ca^{2+} sensitivity of rat myofibrils. J Biol Chem 272:26887–26892
Rosenfeld SS, Taylor EW (1985a) Kinetic studies of calcium and magnesium binding to troponin C. J Biol Chem 260:242–251
Rosenfeld SS, Taylor EW (1985b) Kinetic studies of calcium binding to regulatory complexes from skeletal muscle. J Biol Chem 260:252–261
Sheng Z, Pan BS, Miller TE, Potter JD (1992) Isolation, expression, and mutation of a rabbit skeletal muscle cDNA clone for troponin I. J Biol Chem 267:25407–25413
Sia SK, Li MX, Spyracopoulos L, Gagné SM, Liu W, Putkey JA, Sykes BD (1997) NMR structure of cardiac troponin C reveals an unexpected closed regulatory domain. J Biol Chem 272:18216–18221
Smillie LB, Nattriss M (1990) HPLC of peptides and proteins: separation, analysis, and conformation. In: Mant C, Hodges R (eds) Amino acid analyses of proteins and peptides: an overview. CRC Press, Boca Raton, Fla., pp 809–821
Solaro RJ, Rarick HM (1998) Troponin and tropomyosin: proteins that switch on and tune in the activity of cardiac myofilaments. Circ Res 83:471–480
Spyracopoulos L, Li MX, Sia SK, Gagné SM, Chandra M, Solaro RJ, Sykes BD (1997) Calcium-induced structural transition in the regulatory domain of human cardiac troponin C. Biochemistry 36:12138–12146
Spyracopoulos L, McKay RT, Sykes BD (2000) Structure of skeletal troponin-C in complex with skeletal troponin-I 115–131: comparison to cardiac troponin-C-troponin-I 147–163 complex. Biophys J 78:434A
Tripet BP, Van Eyk JE, Hodges RS (1997) Mapping of a second actin-tropomyosin and a second troponin C binding site within the C-terminus of troponin I, and their importance in the Ca^{2+} dependent regulation of muscle contraction. J Mol Biol 271:728–750
Tung CS, Wall ME, Gallagher SC, Trewhella J (2000) A model of troponin-I in complex with troponin-C using hybrid experimental data: the inhibitory region is a beta-hairpin. Protein Sci 9:1312–1326
van Eerd JP, Takahashi K (1975) The amino acid sequence of bovine cardiac troponin-C. Comparison with rabbit skeletal troponin-C. Biochem Biophys Res Commun 64:122–127
Van Eyk JE, Hodges RS (1988) The biological importance of each amino acid residue of the troponin I inhibitory sequence 104–115 in the interaction with troponin C and tropomyosin-actin. J Biol Chem 263:1726–1732
Vassylyev DG, Takeda S, Wakatsuki S, Maeda K, Maeda Y (1998) Crystal structure of troponin C in complex with troponin I

fragment at 2.3-Å resolution. Proc Natl Acad Sci USA 95:4847–4852

Wang X, Li MX, Spyracopoulos L, Beier N, Chandra M, Solaro RJ, Sykes BD (2001) Structure of the C-domain of human cardiac troponin C in complex with the Ca^{2+} sensitizing drug EMD 57033. J Biol Chem 276:25456–25466

Wüthrich K (1986) NMR of proteins and nucleic acids. Wiley, New York

Zhang O, Kay LE, Olivier JP, Forman-Kay JD (1994) Backbone ^{1}H and ^{15}N resonance assignments of the N-terminal SH3 domain of drk in folded and unfolded states using enhanced-sensitivity pulsed field gradient NMR techniques. J Biomol NMR 4:845–858